Received: 20 April 2022 | Revised: 31 August 2022 | Accepted: 6 September 2022

DOI: 10.1002/apj.2832

RESEARCH ARTICLE

Asia-Pacific Journal of Chemical Engineering | Curtin University | WILEY

Activity and stability of castor oil-based microemulsions with cellulose nanocrystals as a carrier for astaxanthin

Chintya Gunarto[1,2,3] | **Alchris Woo Go**[1] | **Yi-Hsu Ju**[1,4,5] | **Artik Elisa Angkawijaya**[4,6] | **Shella Permatasari Santoso**[2,3] | **Aning Ayucitra**[2] | **Felycia E. Soetaredjo**[2,3] | **Suryadi Ismadji**[2,3]

[1]Department of Chemical Engineering, National Taiwan University of Science and Technology, Taipei City, Taiwan

[2]Department of Chemical Engineering, Widya Mandala Surabaya Catholic University, Surabaya, Indonesia

[3]Collaborative Research Center for Sustainable and Zero Waste Industries, Widya Mandala Surabaya Catholic University, Surabaya, Indonesia

[4]Graduate Institute of Applied Science and Technology, National Taiwan University of Science and Technology, Taipei City, Taiwan

[5]Taiwan Building Technology Center, National Taiwan University of Science and Technology, Taipei City, Taiwan

[6]Plant Lipid Research Team, RIKEN Center for Sustainable Resource Science, Yokohama, Japan

Correspondence
Alchris Woo Go and Yi-Hsu Ju, Department of Chemical Engineering, National Taiwan University of Science and Technology, Keelung Road, 10607, Taipei City, Da'an District, Taipei City, Taiwan.
Email: awgo@mail.ntust.edu.tw and yhju@mail.ntust.edu.tw

Funding information
Ministry of Science and Technology of Taiwan, grant/award number: MOST 108-2221-E-011-106; National Taiwan University of Science and Technology, grant/award number: 109O210007/109O410307.

Abstract

Microemulsions (MEs) are explored for its use in various food and drug formulations and applications. It is an amphiphilic material, consisting of oil phase, surfactant mixture, and aqueous phase. Castor oil (CO), which has anti-inflammatory and analgesic activities, was used as the oil-phase in the ME formulations. Stability and activity of CO-based ME were investigated along with the influence of encapsulating astaxanthin as lipophilic drug and the use of cellulose nanocrystals (CNC) as pickering agent. Regression model for predicting hydrodynamic diameter of astaxanthin-load (400 ppm) was explored with predictors being the weight fraction of CO, surfactant mixture, and CNC amount in the ME. Microemulation size is dependent on the oil-phase and amount of drug loaded, with CNC potentially improving the stability of ME with high CO fraction. The concentration at IC_{50} was reduced from 494.47 to 52.25 μl/ml as the fraction of CO in ME formulation increased between 5 and 28 wt.% for free-radical scavenging activity. The same phenomenon was observed for anti-microbial assay, allowing 94.9% and 93.9% inhibition of *Escherichia coli* and *Staphylococcus aureus* growth, respectively. These results confirmed that CO-based MEs are promising as the topical drug delivery, especially as the carrier for the hydrophobic compound.

KEYWORDS

biological activity, carrier, castor oil, cellulose nanocrystals, microemulsion, stability

1 | INTRODUCTION

Microemulsion (ME) has received great attention due to their amphiphilic characteristic, low surface tension, and biological activity.[1] Microemulsions are isotropically stable, transparent,[2] and have hydrodynamic diameters between 20–200 nm.[3] Three main components that comprise a ME include an oil, a surfactant/cosurfactant mixture (S_{mix}), and an aqueous phase. Castor oil (CO), as an oil phase, has been used in formulating MEs due to the high ricinoleic acid content, which has been previously found to have anti-inflammatory and analgesic activities.[4,5] From an earlier report,[6] CO-based ME showed the highest ME formation area around 18% in combination with water and using Tween 80 as surfactant and ethanol as cosurfactant. Large amounts of surfactants (20–90 wt. %) are typically needed in ME formulations.[7] Therefore, the use of an additive to reduce the required surfactant is of interest to increase the fraction of the hydrophobic component (oil).

Cellulose, starch nanocrystals,[8] and nanoparticles[9,10] were employed to reduce the unfavorable effects from using surfactant.[11,12] Cellulose nanocrystal (CNC) is a promising material that can enhance the stability of ME for prolonged storage and even at extreme temperature conditions (−20 to 40°C).[13] The addition of CNC suspension 0.7 wt.% as an aqueous phase into the CO-based ME formulation suppresses the increase in hydrodynamic diameter to only 4.98%, compared to formulations without CNC where the hydrodynamic diameter increase up to 32.48%, during storage.[13]

Regarding the anti-microbial activity, few studies have reported MEs in various materials. Studies by Alkhatib et al.[14] reported ME formulated with ethyl decanoate as oil phase, cremophor EL as a surfactant, transcutol as cosurfactant, and deionized water as water phase, with encapsulation of cephalosporin resulted in higher anti-microbial property compared to ME alone. Another study using glycerol monolaurate as oil, tween 40 as surfactant, ethanol as a co-factor resulted in 99% inhibition of microbial.[1] However, it is unclear from the aforementioned studies as to the actual or is synergistic contribution of the components in the observed anti-microbial activities. This requires careful investigations of the contribution of component materials used in formulated MEs. Nevertheless, the reported results provide positive insights on the add-value of MEs when used as a medium for drug delivery.

Previous studies on various ME have investigated the encapsulation of hydrophobic drugs such as cephalosporin,[14] levofloxacin,[15] piroxicam,[16] irbesartan,[17] herbal medicine,[18] and also astaxanthin[6] into the ME. Astaxanthin (ASX) is an active compound used as a topical application and has exhibited protective activity against ultraviolet radiation.[19] However, ASX has low bioavailability, low solubility in water, thus requiring a carrier for delivery. Several studies showed encapsulation of ASX with liposomes,[19] hydrogel or lipogel,[20] and ME,[6] as listed in Table 1. The activity of ASX loaded into ME has not been explored. Also, incorporating various ASX concentrations may affect the hydrodynamic diameter of ME and would need to be looked into since it is an essential characteristic of MEs to ensure that the final formulation containing the active agent remains to be a ME.

In an earlier work on formulating CO-based ME, the composition of 5 wt.% CO, 85 wt.% of S_{mix}, and 10 wt.% of deionized water or CNC suspension have been found to have a stable hydrodynamic diameter over 90 days.[6,13] However, formulation and characterization of ME with different CO compositions have not been explored. To develop a better understanding of the CO-based ME, the composition of MEs was formulated with different amounts of CO, tween 80/ethanol, and with two types of aqueous phase: deionized water and CNC suspension

TABLE 1 Release studies condition of ASX in the previous study

Matrix system	Drug release technique adapted	Release condition					Ref
		Medium	pH	T, °C	Time, h	Cumulative ASX release, %	
Nanostructured lipid carrier	Dialysis bag	EtOH/water (1/1, v/v)	-	37	24	88	21
Nanoliposomes	Dialysis bag	PBS[a]	7.4	37	24	28.74	22
Oleoresin-Lipogel Oleoresin-Hydrogel	Dialysis bag	PBS/EtOH (7/3, v/v)	7.4	37	24	20 18	20
Nanoemulsion (.15 wt.% ASX, 4.2 wt.% Caprylic/Capric triglycerides, 2.6 wt.% T80, 1.3 wt.% ascorbyl palmitate, 2 wt.% glycerine, and 89.75 wt.% DI water)	Franz diffusion cell	PBS	7.4	37	4	23.6	23

[a]Phosphate buffer saline.

0.7 wt.%, which were subsequently loaded with different amounts of ASX. This study was aimed to evaluate the hydrodynamic diameter, stability of various CO-based ME formulated with tween 80 and ethanol at a ratio of 2, as surfactant mixture. The free-radical scavenging and anti-microbial activity of selected MEs with and without ASX were also determined.

2 | MATERIALS AND METHODS

2.1 | Materials

CO, and Tween® 80 (T80) as the surfactant were obtained from Sigma-Aldrich (India and USA) along with Ethanol (99.5%) supplied by Echo Chemical (Taiwan), and Astaxanthin (>97%) purchased from Acros (China) was used in the formulation of various MEs. 2,2-diphenyl-1-picrylhydrazyl (DPPH) from Sigma-Aldrich (Germany) was used in the determination of the free-radical scavenging activity of the formulated MEs. Tryptone, Tryptic Soy Broth (TSB) by BD (France), yeast extract from Scharlau (Spain), and sodium chloride (NaCl, 99.5%, Showa, Japan) were used in the preparation of fermentation media for the anti-microbial assay.

2.2 | Preparation of microemulsions

In the preparation of the MEs, a mixture of the surfactant and the cosurfactant (S_{mix}) was first prepared at a fixed weight ratio of 2.[6] CO was then added into the S_{mix}, and thoroughly mixed with an aid of a Vortex Mixer (Scientific, Vortex Genie II) for 30 s, followed by the addition of the aqueous phase (AP) at predetermined weight ratios. Two types of AP were used in this study, deionized water and an aqueous suspension containing 0.7 wt.% CNC. A summary of the formulations adopted and investigated in this work is presented in Figure 1, with the selected formulations located within the ME region.

2.3 | Preparation of cellulose nanocrystals

Cellulose nanocrystals used in this study were prepared according to Putro and colleagues.[24] Filter paper (Whatman No. 2), cut into small pieces, was suspended in water at 65°C and continuously stirred at 350 rpm for 3 h. One gram of the collected cellulose fibers was immediately acid hydrolyzed using 20-ml H_2SO_4 (64 wt.%) for 1 h. After hydrolysis, the partially hydrolyzed solids were collected after subjecting the mixture to centrifugation.

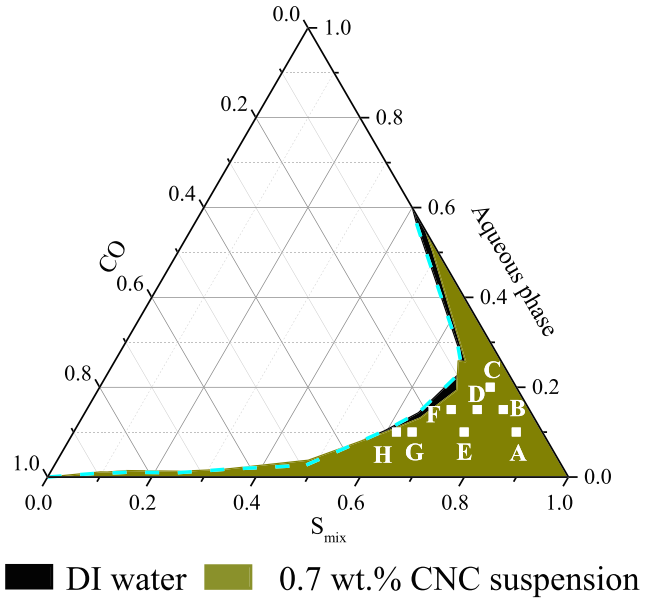

FIGURE 1 Location of different microemulsion (ME) formulation in the pseudo-ternary phase diagram of CO, tween 80/ethanol = 2 as S_{mix}, and aqueous phase, formulated within the ME region based on previously determined and reported data[6,13]

The collected solids were further washed with water to remove the entrained and residual acids. A dialysis bag (12–14 kDa) was used to facilitate the washing while separating the collected solids from the bulk fluid. Washing was repeatedly carried out until the pH of the wash water was ~5.1. The washed partially hydrolyzed and washed solids collected, hereinafter referred to as CNC were refrigerated at −20°C, and freeze-dried.

2.4 | Physicochemical characteristics and storage stability tests

The characterization of ME was limited to the hydrodynamic diameter, polydispersity index, and zeta potential. The stability of MEs during storage was investigated by subjecting the formulated MEs to heating–cooling cycles, freeze–thaw cycles, and induced gravitational acceleration while monitoring the changes in the hydrodynamic diameter, polydispersity index, and zeta potential. About 10 g of ME based on different formulations were prepared for each analysis.

2.4.1 | Hydrodynamic diameter, zeta potential, and polydispersity index

Measurement of hydrodynamic diameter and polydispersity index was done using Zetasizer Nano-S90, Malvern

at 25°C at a fixed angle of 90°. Samples were diluted 100-fold with deionized water to avoid multiple scattering. Zeta potential was determined by ZetaPALS, Brookhaven at 25°C with 30 cycles for each sample. All analyses were conducted in triplicate for each condition. As a control for the subsequent stability tests, samples made adopting the different formulations were stored at 30°C and measured the above-mentioned properties at two-day intervals, over the period of the storage stability test (48 days).

2.4.2 | Heating–cooling stability test

Microemulsion samples were subjected to heating and cooling cycles, which each cycle requiring the sample to be stored at 40°C and 4°C, for 48 h at each temperature. The samples were repeatedly exposed to such conditions for six cycles with the samples measured of their hydrodynamic diameter, polydispersity index, and zeta potential. Samples were allowed to equilibrate to 30°C between temperatures prior to any property measurements. The percentage change of a measured property at a given point of the heating–cooling cycles was expressed relative to the measured property prior to subjecting the samples to the heating–cooling cycles.

2.4.3 | Freeze–thaw stability test

After the samples went through the heat-cooling cycles and measurement of hydrodynamic diameter, zeta potential, and polydispersity index, these were also ocularly inspected. Samples that did not show any separation and color change were further subjected to a freeze–thaw cycle. The samples were placed at −20°C and 25°C, alternately, for 48 h at each temperature, for six cycles. The hydrodynamic diameter was measured at each temperature transition. Apart from samples previously subjected to heating–cooling cycles, fresh samples were prepared and subjected to the freeze–thaw cycles.

2.4.4 | Centrifugal stability test (induced gravitational separation)

The samples that not separate from the previous test proceeded to the centrifugal stability test, which induced the gravitational separation. Centrifugation test was performed at 7920 xg for 5 h, with ocular inspection at every hour to check for possible phase separation. The induced centrifugal force corresponds to 1 year of gravitational pull on the ME during storage.[25]

2.5 | Activity assays

ME biological activities were determined by the free-radical scavenging and microbial inhibition values. Four types of samples: ME only, ME-CNC, ME@ASX, and ME-CNC@ASX in various formulation compositions were compared.

2.5.1 | Free-radical scavenging activity

Free-radical scavenging of various MEs was assessed using 2,2-diphenyl-1-picrylhydrazyl (DPPH) with some modification.[26,27] Different ME suspended in ethanol with different concentrations was added with 0.6 ml of DPPH solution (0.25 mM in ethanol) with the final mixture having a final concentration of 5, 10, 25, 50, 100, 150, 200, 300, 400, and 500 µl/ml. The solutions were incubated at 25°C for 30 min in dark conditions and the absorbance was determined at 517 nm by UV/Vis Spectrophotometer (UV-2600, Shimadzu, Japan).

2.5.2 | Anti-microbial activity assay

Two types of bacteria, gram-negative (*Escherichia coli, E. coli*) and gram-positive (*Staphylococcus aureus, S. aureus*) were used against all ME formulations. *E. coli* was cultured in *Lysogeny Broth* (LB) medium (10-g/L tryptone, 5 g/L of yeast extract, and 10-g/L NaCl), while *S. aureus* was cultured in TSB (30 g/L) medium at 37°C. The absorbance of culture was observed and adjusted to an optical density at 600 (OD_{600}) = 0.5 with subjected medium (microbial culture).

The anti-microbial activity assay was conducted by diluting samples into the medium with a concentration of 75 µl/ml in the flask using the medium solution. Subsequently, microbial suspension (10% v/v) was added to the initial solution, then incubated at 37°C. The aliquots were taken at the predetermined time, and the OD_{600} was observed by UV/Vis Spectrophotometer (UV-2600, Shimadzu, Japan).

2.6 | Statistical and regression analysis

The statistical data analysis was carried out by one-way analysis of variance (ANOVA) and Tukey test using Minitab 17. All experiments were carried out in replicates, and results are reported as the average value of the measured responses along with its standard deviation. Regression analysis was carried out for the determined hydrodynamic diameter of the different ME formulations

loaded with ASX (400 μg/ml), excluding formulation D (CO10-SM75-AP15). The weight fraction of CO (X_1), S_{mix} (X_2), and CNC (X_3) were considered as the variables having the main effects with water excluded since water is a dependent variable relative to the other three components. A multivariate model (Equation 1) was adopted for the regression analysis carried out using Microsoft Excel's data analysis tool, with 40 data points regressed and with MEs based on formulation CO10-SM75-AP15 used as validation samples. The best model for hydrodynamic diameter response was chosen based on the p value, R^2, R^2-adjusted, mean absolute error (Equation 2), and mean bias error (Equation 3).

$$Response = \propto_1 X_1 + \propto_2 X_2 + \propto_3 X_3 + \propto_4 X_1 X_1 + \propto_5 X_2 X_2 + \propto_6 X_3 X_3 + \propto_7 X_1 X_2 + \propto_8 X_2 X_3 + \propto_9 X_1 X_3 + \in \quad (1)$$

$$\text{mean absolute error} = \frac{\sum \left| \frac{\text{Predicted} - \text{Measured}}{\text{Measured}} \right|}{\text{Number of data points}} \times 100\% \quad (2)$$

$$\text{mean bias error} = \frac{\sum \frac{\text{Predicted} - \text{Measured}}{\text{Measured}}}{\text{Number of data points}} \times 100\% \quad (3)$$

3 | RESULTS AND DISCUSSION

Pseudoternary phase diagram was plotted to indicate the ME region in the system.[28–31] Eight different formulations of CO-based MEs were prepared according to the composition aforementioned and indicated in Figure 1, with two types of aqueous phase, deionized water, and 0.7 wt.% CNC suspension. Although having a transparent solution is often the first indicator in formulating MEs,[13] the hydrodynamic diameter (HD) is also an important parameter to ensure that MEs are successfully formulated, which is normally found between 20–200 nm.[3] To confirm the formation of ME, the HD of the different ME were determined and presented in Figure 2. Generally, all MEs have hydrodynamic diameters less than 200 nm, with formulations near the boundary of the ME region having tendencies to exceed 200 nm and formulations with CNC having lower HD. Higher CO amount in the ME resulted in higher HD values. This is in agreement with the study from Sood et al.,[32] by using Captex 500 as an oil phase, the hydrodynamic diameter also increases with a higher oil phase.

Hydrodynamic diameter is a critical parameter from the point of characterizing a ME, as ME with lower HD are often more stable.[33] From the formulated MEs, formulations with higher surfactant (A) and lower CO (A, B, and C) tend to have lower HD and correspondingly have negative and higher zeta potentials (−12.14 to −13.31 mV), especially for those with CNC (−12.86 to −16.06 mV), indicating their tendency to have better stability.[34–36] To better understand the applicability of formulated CO-based MEs, the following section details their use as an encapsulating agent or carrier material for ASX, microbial activity, free-radical scavenging activity, and storage stability.

3.1 | Effect of astaxanthin loading on CO-based microemulsions

In the formulation of ME, the active agent is typically not included and is only added after the ME has been formulated. To determine the influence of loading ASX on the formulated CO-based MEs, ASX was loaded into the MEs with resulting ASX concentrations in the MEs from 200, 400, 600, 800, 1000, and 2000 μg/ml. As could be observed from Figure 2, higher ASX loading increases the HD, especially for ME having low CO (5 wt.%). However, the presence of CNC as part of the formulation results in a lower increase in HD with the addition of ASX (Figure 2a–c). The presence of CNC tends to serve as an additional surfactant and stabilizer, which suppresses the HD of the ME as previously observed for CO-based MEs formulated with 5 wt.%.[13] In view of formulations having higher CO (10–28 wt.%), the addition of ASX did not drastically increase the hydrodynamic diameter (Figure 2d–h). The observed slower increase in the HD could be attributed to the better solubility of ASX in CO as compared to the aqueous phase, with high CO in ME formulation having a better capacity to be loaded with ASX. Considering that MEs are often characterized to have a HD of ≤200 nm, subsequent experiments were conducted with ASX loaded at a concentration of 400 μg/ml in the MEs (except 28 wt.% CO—Formulation H).

3.2 | Effects of microemulsion formulation on the hydrodynamic diameter

The smallest and largest hydrodynamic diameter among ASX-loaded ME were CO5-SM75-AP20 (120.57 nm) and CO28-SM62-AP10 (222.50 nm) at 400-μg/ml ASX. For formulation with CNC-modified ME, the smallest and largest HD were 106.07 and 197.10 nm for ME formulations CO5-SM85-AP10 (A) and CO28-SM62-AP10 (H),

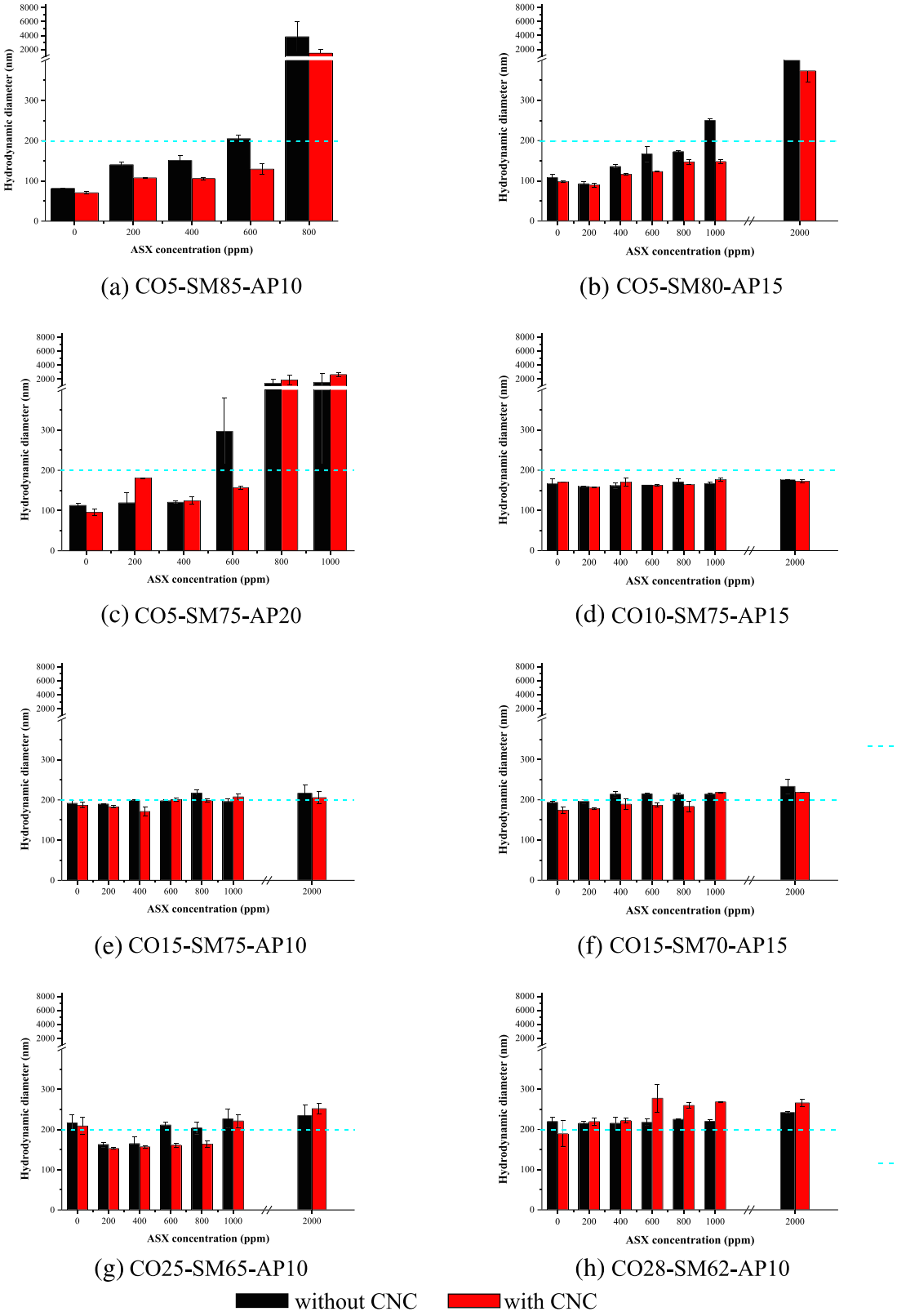

FIGURE 2 (a–h) Hydrodynamic diameter of microemulsion (ME) formulations with different ASX concentration loading

respectively. To aid a better understanding of the effect of CO, S_{mix}, and AP compositions on the resulting HD, the obtained results for MEs (Formulations A to H, except D) loaded with ASX (400 μg/ml) were regressed with a multivariate model, with the regression results summarized in Table 2. A multivariate model with X_1, X_2, and X_3 as

TABLE 2 Summary of regression analysis of the hydrodynamic diameter

Parameters	Regression model[a]: $Y = \alpha_1X_1 + \alpha_2X_2 + \alpha_3X_3 + \alpha_4X_1X_1 + \alpha_5X_2X_2 + \alpha_6X_3X_3 + \alpha_7X_1X_2 + \alpha_8X_2X_3 + \alpha_9X_1X_3 \pm SEE$; range of data: X_1 (.0485–.2805), X_2 (.6205–.8518), X_3 (0–.0014)											
	Linear		Truncated model 1		Linear + interaction		Quadratic		Quadratic − intercept		Truncated model 2	
Predictors[a]	Coefficient	*p* value	Coefficient	*p* value	Coefficient	*p* value	Coefficient	*p* value	Coefficient	*p* value	Coefficient	*p* value
Intercept	90.6757	.5049	0	n.a	0	n.a	312.9443	.0001	0	n.a.	0	n.a.
Linear												
X_1	475.2917	.0010	−1513.5885	.0021	−1735.0742	.0005					−1490.11	.0026
X_2	37.4234	.8145	87.4509	1.85×10^{-7}	83.1449	5.77×10^{-06}					82.0084	1.60×10^{-05}
X_3	−11301.7	.2617			350907.34	.0247					10686.94	.4104
Quadratic												
X_1X_1							345.8533	.4416	2114.7055	7.3×10^{-13}		
X_2X_2							--248.603	.0312	222.4260	3.45×10^{-16}		
X_3X_3							-1.9×10^{7}	.0644	−2171001.49	.8435		
Interaction												
X_1X_2			3384.7562	5.68×10^{-5}	3791.2872	9.18×10^{-06}					3423.1900	6.08×10^{-05}
X_2X_3					−423780.27	.0286					−146013.85	.1507
X_1X_3					−404293.29	.0094						
Standard error of estimate	29.1080	-	23.4547	-	22.0127	-	32.5513		39.4360		23.3045	-
Model ($n = 40$)	-	3.85×10^{-09}	-	4.22×10^{-33}	-	2.29×10^{-30}	-	2.04×10^{-7}	-	5.61×10^{-25}	-	1.04×10^{-30}
Regression												
Degrees of freedom	3	-	3	-	6	-	3	-	3	-	5	-
SS	66277.74	-	1339963.98	-	1343843.45	-	58634.5363	-	1302776.11	-	1341309.98	-
Mean squares	22092.58	-	446654.66	-	223973.91	-	19544.8454	-	434258.7047	-	268,262	-
Residual												
Degrees of Freedom	36	-	37	-	34	-	36	-	37	-	35	-
SS	30501.85	-	20354.47	-	16475.0043	-	38145.0603	-	57542.3361	-	19008.4689	-
MS	847.2737	-	550.1208	-	484.5590	-	10059.5850	-	1555.1983	-	543.0991	-
R^2	.6848	-	.9850	-	.9939	-	.6059	-	.9577	-	.9860	-
R^2-adjusted	.6586	-	.9572	-	.9567	-	.5730	-	.9284	-	.9586	-
Mean absolute error	13.3304	-	11.3222	-	9.3380	-	33.0887	-	18.3691	-	11.1925	
Mean bias error	2.4327	-	1.2263	-	1.0725	-	−9.0579	-	3.0829	-	1.17322	

[a]Response and predictors, Y—hydrodynamic diameter; X_1—weight fraction of castor oil; X_2—weight fraction of S_{mix}; X_3—weight fraction of CNC.

linear predictors, and X_1X_2 & X_2X_3 interaction terms were found to best describe the HD with the highest R^2-adjusted of 0.9586 (Equation 4). Although the inclusion of X_1X_3 interaction terms (Equation 5) also resulted in a good fit ($R^2 = 0.9939$), the R^2-adjusted (0.9567) was not improved, when compared to Equation (4).

$$HD\,(\text{nm}) = -1490.11X_1 + 82.01X_2 + 10686.94X_3 + 3423.19X_1X_2 - 146013.85X_2X_3 \pm 23.30 \quad (4)$$

$$HD\,(\text{nm}) = -1735.07X_1 + 83.14X_2 + 350907.34X_3 + 3791.29X_1X_2 - 423780.27X_2X_3 - 404293.29X_1X_3 \pm 22.01 \quad (5)$$

The coefficient of linear of the predictors indicates how the individual components influence the resulting HD of the ME suspended in water. In principle, if oil is properly dispersed in water, it is possible to produce a dispersion with infinitely small oil droplets owing to their immiscibility; thus, the observed negative coefficient or contribution in the HD. As for the S_{mix}, which is comprised of water-miscible and soluble components, its contribution in the average HD is the least and is observed to be positive probably owing to the larger molecules of T80, which is the main emulsifier that tends to attract water molecules. In the case of CNC addition, CNC is an insoluble material of nano-scale, and would in itself have a specific HD that contributes to the average HD measured. Considering only the coefficients of the main effects may at first glance be contradictory to the trend observed in Figure 2, where higher CO results in higher HD and higher S_{mix} & CNC addition leads to lower HD. However, accounting for the interaction effects between CO-S_{mix}, S_{mix}-CNC, and CO-CNC, the positive coefficient of the interaction term for CO-S_{mix} indicates that the increase in both CO and S_{mix} will indeed bring about an increase in HD as droplets of micelles are formed and dispersed. However, an increase in both is practically not possible, and their change in proportion is in principle inversely proportional, thus, resulting in a lesser overall contribution to the increase in HD. Accounting for the presence of CNC in the mixture interaction with other components results in the decrease in the HD as indicated in Equations (4) and (5) as well as from the observed trends in Figure 2. This is probably owing to the difference in the mechanism in forming an emulsion brought about by the S_{mix} being an emulsifier and that by CNC as a pickering agent. Part of the mechanism of CNC to aid the formation of ME may be owing to its absorptive capacity, whereby components of the mixture are absorbed into the CNC particles and thus decreasing the effective HD. The schematic synergistic effect of hydrodynamic diameter can be seen in Figure S1. Comparing the predicted and measured HD both Equations (4) and (5) allow the prediction of the HD at a good accuracy with low mean absolute error (11.19 and 9.34) and mean bias error (1.17 and 1.07) (Table 2). Further, to evaluate the practical use of the developed models, an additional ME formulation (CO10-AM75-AP15—Formulation D) was prepared and the models were used to predict the HD. Both Equations (4) and (5) can accurately predict the HD of Formulation D with mean absolute error of 6.41 and 7.57, and mean bias error of 2.41, and 4.08, respectively.

3.3 | Free-radical scavenging activity of castor oil-based microemulsions

The CO-based MEs, CO, and ASX solution were determined of its free-radical scavenging activity by adopting DPPH assay, with the corresponding determined IC_{50} presented in Table 3. The absorbance of the DPPH solution at 517 nm decreases as the formulations donate hydrogen ions, thus reducing the free-radical of DPPH into a stable form, which is colorless in color. The highest and lowest IC_{50} were 366.44 and 57.61 μl/ml without CNC addition, 494.47 to 52.25 μl/ml with CNC addition, 384.47 to 70.72 μl/ml for 400 μg/ml ASX in the ME, and 357.86 to 64.43 μl/ml of formulations with the addition of CNC and ASX. Microemulsions at 5 wt.% of CO with different S_{mix} and AP weight ratios had a similar value of IC_{50}. The CO and ASX solution activity were observed individually to identify the cause of inhibition, either from the actual or synergistic effect of MEs. It is expected that the IC_{50} is lower with ME formulations having high CO as oil phase considering that pure CO only requires a concentration of 15.03 μl/ml to achieve 50% inhibition. Consistently, formulations with higher CO had the lowest IC_{50} among CO-based ME. The addition of CNC generally does not contribute to the free-radical scavenging activity. The activity of pure CNC suspension was not observed within the range tested. Criado et al.[37] also reported that the free-radical scavenging activity of CNC is low and increased when higher CNC concentration (10 wt.%) was introduced. Furthermore, the IC_{50} for some formulations did not show significant changes after the addition of ASX. This agrees with the low inhibition of ASX solution (400 μg/ml in ethanol), 479.92 μl/ml.[38] CO contains high ricinoleic acid (>80%) and flavonoid compounds that donate hydrogen ions and possess high radical scavenging activity.[39] CO-based ME not only serves as a carrier for lipophilic drug delivery but could also provide additional protection from free radicals.

TABLE 3 Free-radical scavenging activity for various ME formulation and its component materials expressed in concentration at IC_{50}[a]

	Concentration at IC_{50} (μl/ml)			
Formulation/material	**ME without CNC**	**ME-CNC**	**ME@ASX**	**ME-CNC@ASX**
CO5-SM75-AP20	346.43 ± 36.28^{d}	494.47 ± 3.54^{a}	384.48 ± 42.53^{cd}	357.86 ± 2.76^{d}
CO5-SM80-AP15	366.44 ± 18.31^{d}	437.17 ± 5.08^{bc}	n.d.[b]	n.d.[b]
CO5-SM85-AP10	349.22 ± 5.75^{d}	479.66 ± 2.76^{ab}	n.d.[b]	n.d.[b]
CO10-SM75-AP15	179.77 ± 9.52^{e}	185.05 ± 2.05^{e}	136.66 ± 5.46^{ef}	135.24 ± 4.60^{ef}
CO15-SM75-AP10	119.24 ± 22.78^{g}	120.10 ± 1.90^{g}	115.33 ± 5.75^{h}	107.00 ± 5.33^{i}
CO15-SM70-AP15	107.96 ± 2.51^{i}	120.71 ± 5.69^{g}	108.19 ± 6.07^{i}	113.28 ± .18^{h}
CO25-SM65-AP10	64.98 ± 3.37^{j}	68.28 ± 5.18^{j}	70.72 ± 4.89^{j}	64.43 ± 2.34^{j}
CO28-SM62-AP10	57.61 ± 6.60^{j}	52.25 ± 1.46^{j}	n.d.[b]	n.d.[b]
Astaxanthin solution[c]	479.92 ± 21.41			
Castor oil	15.03 ± .90			

[a]Average values of IC_{50} followed by the same letters indicate no significant difference ($p > .05$) between values.
[b]n.d.: not determined.
[c]400 μg/ml of ASX in ethanol.

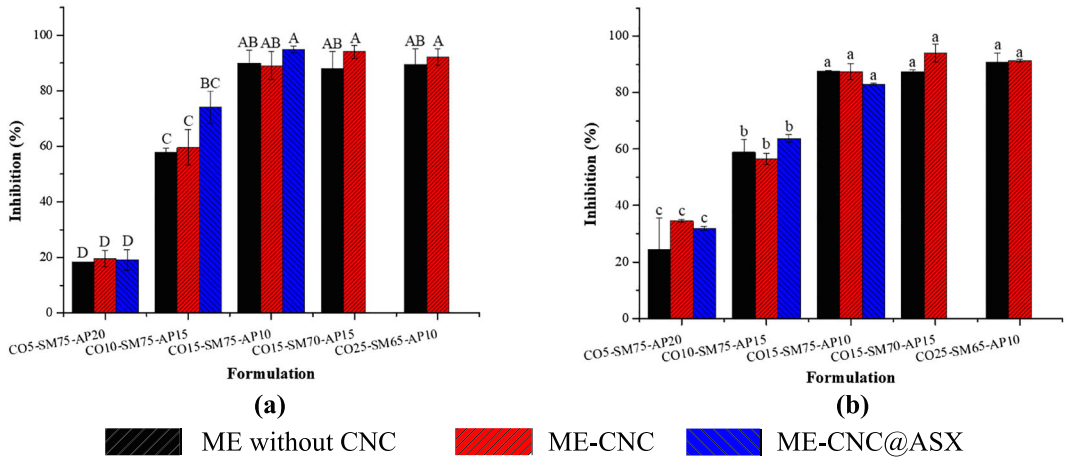

FIGURE 3 Inhibition (%) of microemulsion (ME) only, ME-cellulose nanocrystals (CNC), and ME-CNC@ASX with various formulation toward (a) *Escherichia coli* and (b) *Staphylococcus aureus*. Different letters indicate significant differences among the formulation.

3.4 | Anti-microbial activity of CO-based microemulsions

Based on the insignificant differences in free-radical scavenging activity for formulations with the same CO amount, formulations CO5-SM75-AP20, CO10-SM75-AP15, CO15-SM75-AP10, CO15-SM70-AP15, and CO25-SM65-AP10 were selected and further assayed for their anti-microbial activity. From the results of the assay present in Figure 3, it is evident that the formulations tested had anti-microbial activity against *E. coli* and *S. aureus*. For the growth inhibition of *E. coli* after 16 h of incubation, the inhibitory effect was enhanced with higher CO in the formulation, from 18.49% to 90.06% on ME without CNC, 19.67% to 94.06% on ME-CNC addition, and 19.18 to 94.89% of ME-CNC@ASX as CO increased from 5 wt.% to 25 wt.% in the ME. A similar inhibitory activity was observed in the microbial assays involving gram-positive microbe, *S. Aureus* incubated for 24 h, from 24.35 to 90.66% for ME without CNC, 34.52 to 93.90% for ME-CNC, and 31.91 to 83.02% for ME-CNC with ASX encapsulated. However, ME without CNC resulted in higher inhibition toward *S. aureus* compared to *E. coli* due to the outer lipid membrane present in gram-positive microbes and affected their morphology and the composition of cell wall.[14]

The presence of CO in the ME is suspected to have resulted in the growth inhibition of *S. aureus* and *E. coli*, as supported by the increased inhibition along with increasing CO in formulated MEs. To confirm that the

activity is mainly owing to CO, the inhibitory effect of other components was also tested. The inhibition brought about by the equivalent amount of S_{mix} at 75 wt.% in the ME is 16.01 ± 0.87% and 26.25 ± 2.80% for *E. coli* and *S. aureus*, respectively. Inhibition of ME formulated with and without CNC was not significantly different ($p > 0.05$). The ricinoleic fatty acid existed in the CO is the main cause of microbial inhibition.[40] CO-based MEs-formulated has anti-microbial activity and practical application as topical drug delivery.

3.5 | Stability of CO-based microemulsions

With the observations made earlier on the free-radical scavenging and anti-microbial activity exhibited by the different MEs, higher CO in the formulated ME results in enhanced biological activities. However, high quantities of oil in the ME significantly reduces its shelf-life, thus, it would be imperative to verify and ensuring that the formulated ME is stable.[41] Formulations CO5-SM75-AP20, CO10-SM75-AP15, CO15-SM75-AP10, CO15-SM70-AP15, and CO25-SM65-AP10 were further investigated for their stability by monitoring their HD, PDI, and zeta potential over a period of 48 days. From the gathered results it could be observed that the HD of the heating–cooling cycle for MEs without CNC addition with 5 wt.% CO (CO5-SM75-AP20) changed from 85.35 ± 1.83 to 114.5 ± 9.09 nm while MEs with higher CO (10 and 15 wt.%), the HD was fluctuated between 142.13 ± 4.09 to 181.70 ± 6.11 nm and 181.50 ± 6.25 to 234.7 ± 15.82 nm, respectively. However, a significant increase in HD was observed for CO25-SM65-AP10 formulation, from 255.70 ± 20.79 to 449.83 ± 41.09 nm after the heating–cooling cycle period of 24 days (Figure 4a) and then reached 489.93 ± 26.11 nm after the freeze–thaw cycle period of 24 days (Figure 4c). Interestingly, the addition of 0.7 wt.% CNC in ME with high CO (CO25-SM65-AP10) stabilizes it and suppresses the change HD during both heat-cool and freeze–thaw cycles as shown in Figures 4b and 4d. These results in

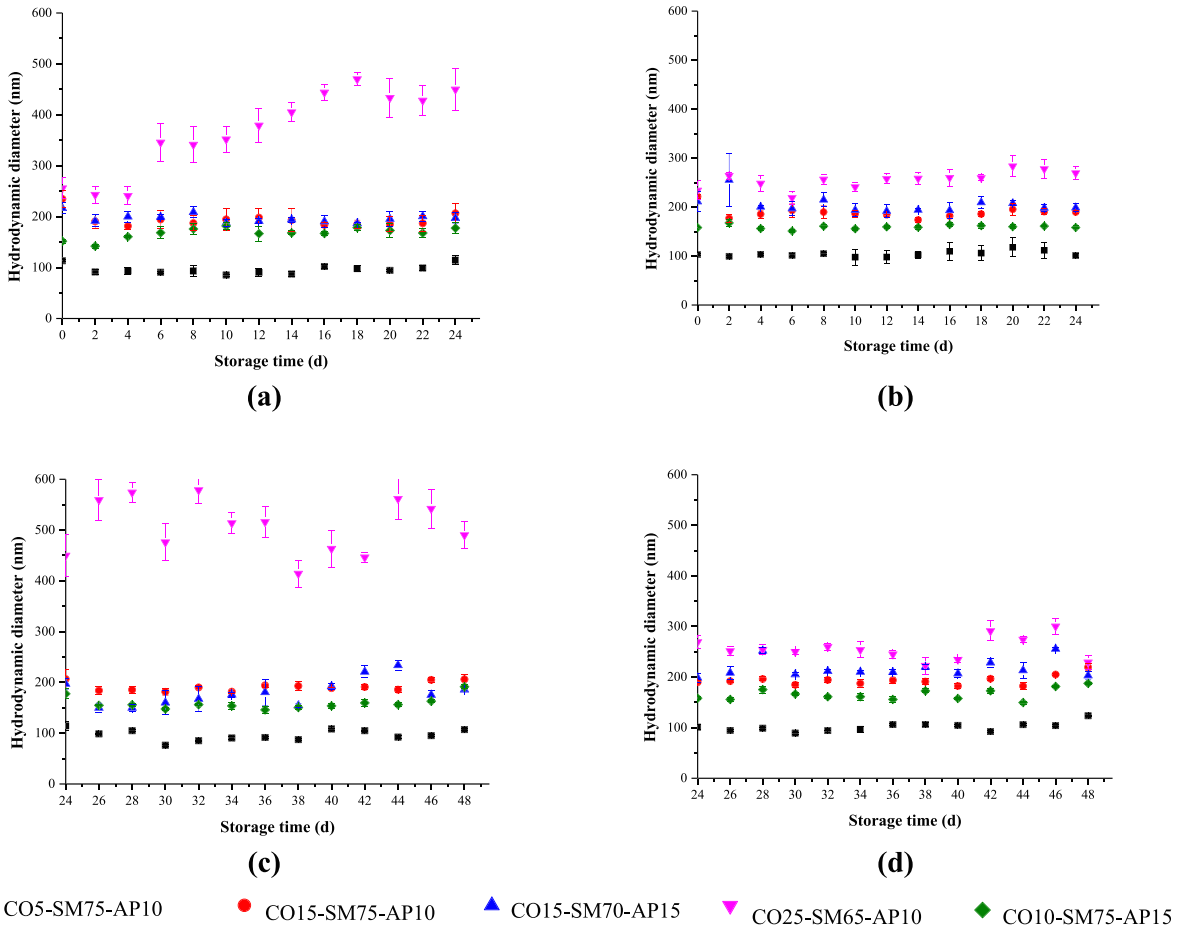

FIGURE 4 The hydrodynamic diameter of microemulsion (ME) formulation through heating–cooling cycle for 24 days for formulation (a) without cellulose nanocrystals (CNC) and (b) with CNC; followed by freeze–thaw cycle for 24 days for formulation (c) without CNC and (d) with CNC

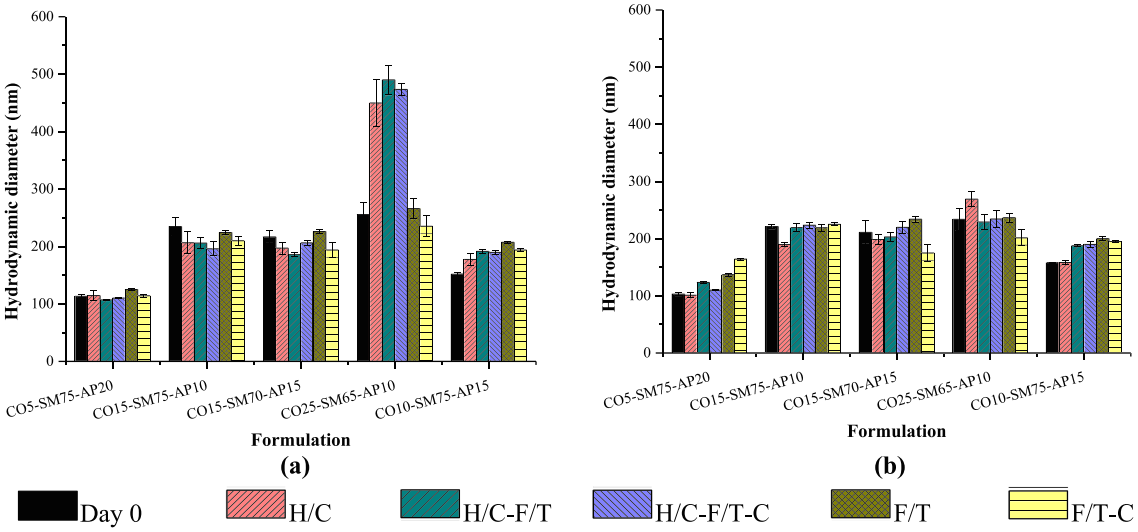

FIGURE 5 Hydrodynamic diameter of various microemulsion (ME) formulations at day 0, heating–cooling cycle (H-C), heating–cooling/freeze–thaw cycles (H-C/F-T), heating–cooling/freeze–thaw/centrifugation (H-C/F-T/C), freeze–thaw cycle (F-T), and freeze–thaw/centrifugation (F-T/C) without CNC (a), and ME-CNC (b).

agreement with observations made in a previous study, where the addition of CNC improved the stability of MEs during storage.[13] The HD of the control (kept at 30°C) formulations were more stable, especially for formulation with 25 wt.% CO which has a similar HD value with formulation using CNC addition through heating–cooling cycle. This implies that CNC helps the stability of ME to become less sensitive to changes in HD at high temperatures. Comparison of HD trends between heating–cooling cycle and control (kept at 30°C) also freeze–thaw cycle and control could be found in Figures S2 and S3.

Presented in Figure 5 the HD of various ME formulations at day 0, heating–cooling cycle (H-C), heating–cooling/freeze–thaw cycles (H-C/F-T), heating–cooling/freeze–thaw/centrifugation (H-C/F-T/C), freeze–thaw cycle (F-T), and freeze–thaw/centrifugation (F-T/C) with and without CNC. As could be observed, CO25-SM65-AP10 formulation with 25 wt.% CO, which underwent F-T cycle only had a lower HD when compared to those that have undergone the H-C/F-T cycle. From these results, it may be inferred that storage at high temperature (~40°C) significantly increases the HD, and storage of ME would best be done at room temperature (30°C) or under cold conditions (−20°C) to avoid drastic changes in the HD. Storage at high temperature results in the increase of HD, accompanied by smaller zeta potential compared to those stored at room temperature. Polydispersity index and zeta potential values of various ME formulations before and after the H-C cycle, H-C/F-T cycles, and H-C/F-T/C are listed in Table S1. All MEs in this study have PDI less than 0.5 indicating homogeneous and stable formulations.[42] The zeta potential values range from −4.55 to −17.97 mV and −6.06 to −22.44 mV for ME without and with CNC, respectively. Tween 80 as a nonionic surfactant and hydroxyl group of CO as oil phase contributed to the negative surface charge in the CO-based MEs.[6] Compared to HD, zeta potential and PDI of MEs are stable and did not significantly change over the 48-days storage period. However, the higher zeta potential of ME formulations with CNC imply better stability than systems without CNC and is supported by the suppressed changes in the HD. Better stability of ME during heat stability is promising for pharmaceutical applications in the future.

4 | CONCLUSIONS

CO-based MEs with various weight ratios of CO, Tween 80/ethanol, and aqueous phase consist of deionized water or 0.7 wt.% CNC suspension has been successfully formulated. Astaxanthin loaded into CO-based ME at 400 μg/ml was found to be the limit to ensure the resulting ME falls within the required HD. The highest and lowest IC_{50} value for free-radical scavenging was 494.47 and 52.25 μl/ml for ME with CNC addition, respectively. The biological activities of ME are enhanced as the fraction of CO in the ME is increased (15 wt.% CO). Moreover, addition of CNC and ASX components in the base ME did not improve the biological activities. However, the addition of CNC improves the storage stability of MEs, especially those with a high (25 wt.%) CO fraction. Microemulsion formulations could potentially be adapted for use as in topical drug delivery systems with its high anti-microbial activity (90.06% for *E. coli* and 90.667% for *S. aureus*).

ACKNOWLEDGEMENTS

This work was financially supported by the Ministry of Science and Technology, Taiwan through the approved research grant, MOST 108-2221-E-011-106. The authors would also like to thank the National Taiwan University of Science and Technology for the teaching and research start-up support and grant (109O210007/109O410307) given to A.W.G. for 2019–2021 to organize the research group involved.

CONFLICT OF INTEREST

The authors declare no conflicts of interest.

ORCID

Artik Elisa Angkawijaya https://orcid.org/0000-0002-4405-5068
Shella Permatasari Santoso https://orcid.org/0000-0003-4698-583X
Aning Ayucitra https://orcid.org/0000-0002-6838-9396

REFERENCES

1. Zhang H, Cui Y, Zhu S, Feng F, Zheng X. Characterization and antimicrobial activity of a pharmaceutical microemulsion. *Int J Pharm*. 2010;395(1-2):154-160. doi:10.1016/j.ijpharm.2010.05.022
2. Nazar MF, Saleem MA, Basharat H, et al. Architecting water dispersible organic nanopowder from volatile microemulsion: an emerging colloidal technology. *Colloids Interface Sci Commun*. 2021;45(September):100536. doi:10.1016/j.colcom.2021.100536
3. Talegaonkar S, Azeem A, Ahmad F, Khar R, Pathan S, Khan Z. Microemulsions a novel approach to enhanced drug delivery. *Recent Pat Drug Deliv Formul*. 2008;2(3):238-257. doi:10.2174/187221108786241679
4. Naik SN, Saxena DK, Dole BR, Khare SK. *Potential and Perspective of Castor Biorefinery*. Elsevier B.V.; 2018. doi:10.1016/B978-0-444-63992-9.00021-5
5. Vieira C, Evangelista S, Cirillo R, Lippi A, Maggi CA, Manzini S. Effect of ricinoleic acid in acute and subchronic experimental models of inflammation. *Mediators Inflamm*. 2000;9(5):223-228. doi:10.1080/09629350020025737
6. Gunarto C, Ju YH, Putro JN, et al. effect of a nonionic surfactant on the pseudoternary phase diagram and stability of microemulsion. *J Chem Eng Data*. 2020;65(8):4024-4033. doi:10.1021/acs.jced.0c00341
7. Yew HC, Misran M. Nonionic mixed surfactant stabilized water in oil microemulsions for active ingredient in vitro sustained release. *J Surfactant Deterg*. 2016;19(1):49-56. doi:10.1007/s11743-015-1753-z
8. Azfaralariff A, Farahfaiqah F, Joe LS, et al. Sago starch nanocrystal stabilized Pickering emulsions Stability and rheological behavior. *Int J Biol Macromol*. 2021;182:197-206. doi:10.1016/j.ijbiomac.2021.03.132
9. Nazar MF, Myakonkaya O, Shah SS, Eastoe J. Separating nanoparticles from microemulsions. *J Colloid Interface Sci*. 2011;354(2):624-629. doi:10.1016/j.jcis.2010.11.017
10. Azfaralariff A, Fazial F, Sontanosamy RS, Nazar M, Lazim A. Food grade particle stabilized pickering emulsion using modified sago (*Metroxylon sagu*) starch nanocrystal. *J Food Eng*. 2020;280(October 2019):109974. doi:10.1016/j.jfoodeng.2020.109974
11. Kalashnikova I, Bizot H, Cathala B, Capron I. Modulation of cellulose nanocrystals amphiphilic properties to stabilize oil water interface. *Biomacromolecules*. 2012;13(1):267-275. doi:10.1021/bm201599j
12. Paximada P, Tsouko E, Kopsahelis N, Koutinas AA, Mandala I. Bacterial cellulose as stabilizer of o w emulsions. *Food Hydrocoll*. 2016;53:225-232. doi:10.1016/j.foodhyd.2014.12.003
13. Gunarto C, Hsu H, Go AW, et al. Effect of cellulose nanocrystal supplementation on the stability of castor oil microemulsion. *J Mol Liq*. 2021;325:115181. doi:10.1016/j.molliq.2020.115181
14. Alkhatib MH, Aly MM, Saleh OA, Gashlan HM. Antibacterial activity of a microemulsion loaded with cephalosporin. *Biol*. 2016;71(7):748-756. doi:10.1515/biolog-2016-0105
15. Nazar MF, Saleem MA, Bajwa SN, et al. encapsulation of antibiotic levofloxacin in biocompatible microemulsion formulation insights from microstructure analysis. *J Phys Chem A*. 2017;121(2):437-443. doi:10.1021/acs.jpcb.6b09326
16. Nazar MF, Khan AM, Shah SS. Microemulsion system with improved loading of piroxicam: a study of microstructure. *AAPS PharmSciTech*. 2009;10(4):1286-1294. doi:10.1208/s12249-009-9328-9
17. Saleem MA, Nazar MF, Siddique MY, et al. Soft templated fabrication of antihypertensive nano Irbesartan Structural and dissolution evaluation. *J Mol Liq*. 2019;292:111388. doi:10.1016/j.molliq.2019.111388
18. Oliveira DAJ, Amaral JG, Garcia LB, et al. Associating chitosan and microemulsion as a topical vehicle for the administration of herbal medicines. *Carbohydr Polym*. 2021;255(June 2020). doi:10.1016/j.carbpol.2020.117482
19. Hama S, Takahashi K, Inai Y, et al. Protective Effects of Topical Application of a Poorly Soluble Antioxidant Astaxanthin Liposomal Formulation on Ultraviolet Induced Skin Damage. *J Pharm Sci*. 2012;101:2909-2916. doi:10.1002/jps
20. Eren B, Tuncay Tanrıverdi S, Aydın Köse F, Özer Ö. Antioxidant properties evaluation of topical astaxanthin formulations as anti aging products. *J Cosmet Dermatol*. 2019;18(1):242-250. doi:10.1111/jocd.12665
21. Mao X, Tian Y, Sun R, Wang Q, Huang J, Xia Q. Stability study and in vitro evaluation of astaxanthin nanostructured lipid carriers in food industry. *Integr Ferroelectr*. 2019;200(1):208-216. doi:10.1080/10584587.2019.1592626
22. Pan L, Wang H, Gu K. Nanoliposomes as vehicles for astaxanthin Characterization, in vitro release evaluation and structure. *Molecules*. 2018;23(11):1-12. doi:10.3390/molecules23112822
23. Fratter A, Biagi D, Cicero AFG. Sublingual delivery of astaxanthin through a novel ascorbyl palmitate based nanoemulsion Preliminary data. *Mar Drugs*. 2019;17(9):1-14. doi:10.3390/md17090508
24. Putro JN, Ismadji S, Gunarto C, et al. the effect of surfactants modification on nanocrystalline cellulose for paclitaxel loading and release study. *J Mol Liq*. 2019;282:407-414. doi:10.1016/j.molliq.2019.03.037

25. Malakar J, Sen SO, Nayak AK, Sen KK. Development and evaluation of microemulsions for transdermal delivery of insulin. *ISRN Pharm*. 2011;2011:1-7. doi:10.5402/2011/780150
26. Navarro-Hoyos M, Alvarado-Corella D, Moreira-Gonzalez I, Arnaez-Serrano E, Monagas-Juan M. Polyphenolic composition and antioxidant activity of aqueous and ethanolic extracts from uncaria tomentosa bark and leaves. *Antioxidants*. 2018;7(5): 1-18. doi:10.3390/antiox7050065
27. Sharma OP, Bhat TK. DPPH antioxidant assay revisited. *Food Chem*. 2009;113(4):1202-1205. doi:10.1016/j.foodchem.2008.08.008
28. Rahman HMAU, Afzal S, Nazar MF, Alvi DA, Khan AM, Asghar MN. Phase behavior of a TX 100 oleic acid water based ternary system: a microstructure study. *J Mol Liq*. 2017;230:15-19. doi:10.1016/j.molliq.2017.01.011
29. Saleem MA, Nazar MF, Yameen B, Khan AM, Hussain SZ, Khalid MR. Structural insights into the microemulsion mediated formation of fluoroquinolone nanoantibiotics. *ChemistrySelect*. 2018;3(41):11616-11621. doi:10.1002/slct.201801925
30. Nazar MF, Mujeed A, Siddique MY, et al. Structural dynamics of tween based microemulsions for antimuscarinic drug mirabegron. *Colloid Polym Sci*. 2020;298(3):263-271. doi:10.1007/s00396-020-04603-w
31. Siddique MY, Alamgir I, Nazar MF, et al. Structural and probing dynamics of Brj 35 based microemulsion for fluoroquinolone antibiotics. *Colloid Polym Sci*. 2021;299(9):1479-1488. doi:10.1007/s00396-021-04871-0
32. Sood J, Sapra B, Tiwary AK. Microemulsion transdermal formulation for simultaneous delivery of valsartan and nifedipine formulation by design. *AAPS PharmSciTech*. 2017;18(6): 1901-1916. doi:10.1208/s12249-016-0658-0
33. Vadlamudi HC, Yalavarthi RP, Rao MB, Sundaresan C. Insights of microemulsions: a thermodynamic comprehension. *Jordan J Pharm Sci*. 2017;10(1):23-40. doi:10.12816/0039539
34. Saleem MA, Yasir Siddique M, Nazar MF, et al. Formation of antihyperlipidemic nano ezetimibe from volatile microemulsion template for enhanced dissolution profile. *Langmuir*. 2020; 36(27):7908-7915. doi:10.1021/acs.langmuir.0c01016
35. Yasir SM, Nazar MF, Mahmood M, et al. Microemulsified gel formulations for topical delivery of clotrimazole structural and in vitro evaluation. *Langmuir*. 2021;37(46):13767-13777. doi:10.1021/acs.langmuir.1c02590
36. Nazar MF, Yasir Siddiqu M, Saleem MA, et al. Fourth generation antibiotic Gatifloxacin encapsulated by microemulsions structural and probing dynamics. *Langmuir*. 2018;34(36): 10603-10612. doi:10.1021/acs.langmuir.8b01775
37. Criado P, Fraschini C, Salmieri S, Becher D, Safrany A, Lacroix M. Evaluation of antioxidant cellulose nanocrystals and applications in gellan gum films. *Ind Biotechnol*. 2015; 11(1):59-68. doi:10.1089/ind.2014.0017
38. Müller L, Fröhlich K, Böhm V. Comparative antioxidant activities of carotenoids measured by ferric reducing antioxidant power (FRAP), ABTS bleaching assay (αTEAC), DPPH assay and peroxyl radical scavenging assay. *Food Chem*. 2011;129(1): 139-148. doi:10.1016/j.foodchem.2011.04.045
39. Yeboah A, Ying S, Lu J, et al. Castor oil (*Ricinus communis*): a review on the chemical composition and physicochemical properties. *Food Sci Technol*. 2020; 1-15. doi:10.1590/fst.19620
40. Persson C, Robert E, Carlsson E, et al. The effect of unsaturated fatty acid and triglyceride oil addition on the mechanical and antibacterial properties of acrylic bone cements. *J Biomater Appl*. 2015;30(3):279-289. doi:10.1177/0885328215581316
41. Ma Q, Davidson PM, Zhong Q. Antimicrobial properties of microemulsions formulated with essential oils, soybean oil, and Tween 80. *Int J Food Microbiol*. 2016;226:20-25. doi:10.1016/j.ijfoodmicro.2016.03.011
42. Dehghani F, Farhadian N, Golmohammadzadeh S, Biriaee A, Ebrahimi M, Karimi M. Preparation, characterization and in vivo evaluation of microemulsions containing tamoxifen citrate anti cancer drug. *Eur J Pharm Sci*. 2017;96:479-489. doi:10.1016/j.ejps.2016.09.033

SUPPORTING INFORMATION

Additional supporting information can be found online in the Supporting Information section at the end of this article.

How to cite this article: Gunarto C, Go AW, Ju Y-H, et al. Activity and stability of castor oil-based microemulsions with cellulose nanocrystals as a carrier for astaxanthin. *Asia-Pac J Chem Eng*. 2022;e2832. doi:10.1002/apj.2832